ICAS-98-3,5,1

A98-31548

REATTACHMENT OF AN INCLINED WALL JET

J.C.S. Lai and D. Lu

School of Aerospace & Mechanical Engineering
University College, The University of New South Wales
Australian Defence Force Academy, Canberra 2600, AUSTRALIA.

ABSTRACT

Despite numerous theoretical and experimental studies of wall jets, the velocity field of an inclined wall jet in the near field has never been fully explored. The complex flow features of an inclined wall jet include the outer and inner shear layers of the jet and the recirculation flow region bounded by the nozzle plate, the wall and the inner shear layer. In this paper, these flow features are illustrated by laser sheet smoke flow visualisation and quantified by hot-wire and LDA measurements for a 30° inclined wall jet with a nozzle exit Reynolds number of 6,700. Comparisons between the hot-wire and LDA measurements indicate that except in the recirculation flow region where hot-wires cannot discriminate against reversed flow, the results are very similar. Reattachment lengths determined by LDA for various inclined wall angles (β) indicate that provided that the nozzle aspect ratio is greater than 30 and β is less than 50°, the reattachment length is independent of the nozzle aspect ratio and the nozzle exit Reynolds number between 6,670 and 13,340. These reattachment lengths determined by LDA show general agreement with those determined using wall surface oil film visualisation technique.

NOMENCLATURE

h	width of two-dimensional nozzle
L	length of inclined wall
l	length of nozzle
R_o	nozzle exit Reynolds number based on h and U_o
U	mean X-component or x-component velocity
U_m	centre-line velocity (maximum X-component velocity at a given X)
U_o	averaged nozzle exit velocity
V	mean Y-component or y-component velocity
u'/U_o	streamwise turbulence intensity
v'/U_o	transverse turbulence intensity
X	streamwise direction in a rectangular Cartesian coordinate system based at the nozzle exit (Figure 1)
Y	transverse direction in a rectangular Cartesian coordinate system based at the nozzle exit (Figure 1)
$Y_{1/2}$	lateral location of jet half-width in the outer shear layer (Fig. 1)
$Y_{-1/2}$	lateral location of jet half-width in the inner shear layer (Fig. 1)
x	streamwise direction in a rectangular Cartesian coordinate system based at the wall (Figure 1)
x_r	reattachment distance measured along the wall from the nozzle
y	streamwise direction in a rectangular Cartesian coordinate system based at the wall (Figure 1)
y_m	location in the y-direction where $U=U_m$
β	wall angle (Figure 1)
θ_o	initial momentum thickness

INTRODUCTION

Turbulent wall jets have been studied both theoretically and experimentally [1]. However, most data were obtained in the far field of the jet where self preservation is being approached. In most practical applications, a jet is injected at an angle to a solid boundary and the region of interest is within the first ten nozzle widths. As shown in Fig. 1, provided that the angle β between the nozzle plate and the wall is large enough, the inclined wall jet would be separated from the wall as soon as it leaves the nozzle and reattaches to the wall at some distance downstream. Inclined wall jets have numerous important engineering applications, such as in advanced aerofoil designs, film cooling of turbine blades, gas turbine combustion chamber walls and deflectors used in air conditioning ducts etc.

Forthmann [2] conducted the first experimental study of an inclined wall jet and the Coanda effect (in which a jet reattaches to a nearby solid surface) has attracted considerable attention [3]. While pressure measurements in an inclined wall jet were reported by Newman [4] and several attempts in modelling the flow to predict the jet reattachment distance were made such as

by Bourque [5] and Perry [6], the velocity field of an inclined wall jet, particularly in the near field, has not been fully explored. Recently, Lai & Lu [7] investigated the effects of the wall angle on the spatial development of an inclined wall jet using constant temperature hot-wire anemometry for β=0°, 15°, 30° and 45°. Although surface pressure measurements and flow visualisation results as documented by Lai & Lu [8] seem to correlate quite well with the hot-wire measurements, the hot-wire data cannot discriminate against reversed flow in the recirculation flow region between the main jet flow and the wall. It is, therefore, essential to use a technique such as laser Doppler anemometry (LDA) to resolve such flow ambiguities.

The objectives of this paper are, therefore,

(i) to document the velocity field of a 30° inclined wall jet using a two-component LDA, which is hitherto not available in the literature;
(ii) to compare the mean flow characteristics of a 30° inclined wall jet obtained by constant temperature hot-wire anemometer with those of LDA; and
(iii) to provide detailed information on the reattachment of a 30° inclined wall jet.

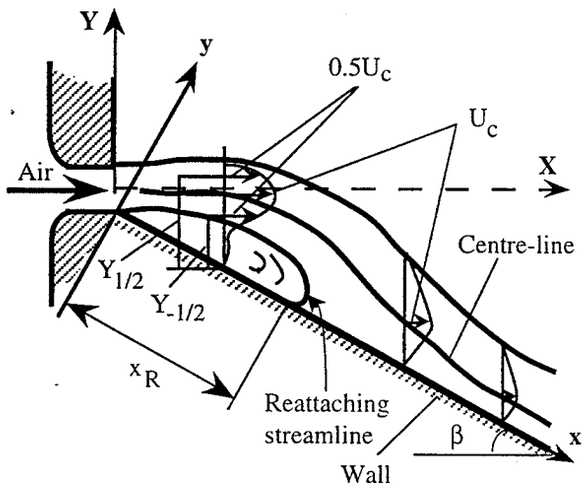

Fig. 1 Schematic of an inclined wall jet flow.

APPARATUS AND INSTRUMENTATION

Apparatus

In the two-dimensional nozzle facility shown schematically in Figure 2, the jet of air was issued into stationary air from a rectangular nozzle with profiles based upon the British Standard BS1042 [9] The nozzle dimensions were: length l =300 mm, width h =5 mm, giving an aspect ratio of 60. The perspex jet settling chamber is 770 mm long, 150 mm wide and 400 mm high. The air flow rate was controlled with a frequency invertor (KVFN 222H Transistor Invertor manufactured by KASUGA E. W. Ltd. Japan) in conjunction with a butterfly valve at the blower inlet, giving various nozzle exit velocities up to 50 m/s. Air from a blower was passed through a series of grids which reduced the turbulence intensity at the nozzle exit for the steady jet to about 0.3 % at the centre-line, as described by Lai & Simmons [10]. The wall length was L=500 mm, giving L/h = 100. The wall angle β was set at 30°. No side plates were used to enhance the two-dimensionality of the flow. Hot-wire and LDA probes, controlled by an NEC 386/20 computer, were traversed in the streamwise and transverse directions by two stepping motors. The smallest step in each direction was 0.015 mm. The nozzle exit Reynolds number (based on nozzle width h and exit velocity (U_o)) was 6,700. The variation of the ambient temperature variation was within ±1°C.

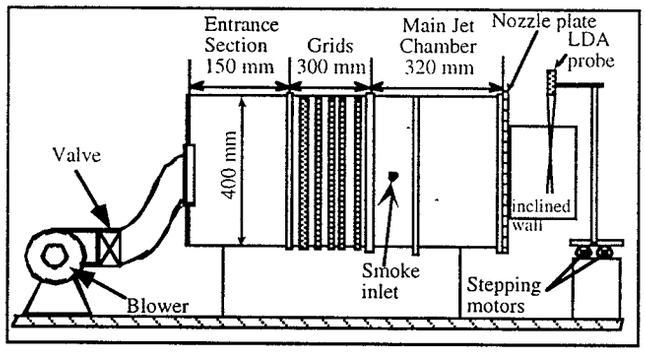

Fig. 2 Schematic diagram of the experimental rig.

Instrumentation

Hot-wire anemometry (HWA) Both single and X hot-wires, operated at an overheat ratio 1.3 with a TSI IFA100 constant temperature anemometer were used to obtain the mean velocities, turbulence intensities and Reynolds stress up to 10 nozzle widths downstream of the nozzle exit. The hot-wire was calibrated at the nozzle exit of the wall jet facility but with the wall removed. A fourth order polynomial fit was applied to the relationship between the output voltage of the hot-wire and velocity measured with a Pitot tube. The angular sensitivity of the X-wire was calibrated in the same facility which allowed the X-wire to be rotated through an angular range from -28° to 28° in steps of 2°, where 0° bisects the X-wire. Except at the edge of the jet and near the wall, the uncertainty in the velocity and turbulence intensity measurements is within 2.5% and 5% respectively.

Laser Doppler anemometry (LDA) The LDA system comprised a Coherent's INNOVA 70 series Argon ion laser and two DANTEC 57N10 Burst Spectrum Analysers (BSA) Each BSA was set to eliminate signals out of the frequency band of interest in order to maximise the signal-to–noise ratio of the Doppler signals. Good quality signals were then detected through a burst detector unit. The burst detector could operate on either the pedestal of the Doppler burst, the envelope of the band-pass filtered or a gated version of the two detector signals. A smoke generator, SMT 1482 Smoke Tunnel (manufactured by Plint & Partners Ltd. England) was used for seeding the flow. The liquid used to produce smoke was non-poisonous Rosco " FOG FLUID " made by Rosco Laboratories INC., USA. Seeding particles

(smoke) were introduced into the flow through both sides of the jet settling chamber as shown in Fig. 2. The Burst Spectrum Analysers were operated in the continuous mode and the number of burst samples for each measurement was at least 2000. The raw velocity data were corrected by applying a weighting function using the time between particle arrivals in order to reduce the velocity bias errors. Detailed description of the BSA circuitry and the data acquisition software can be found in the BSA manual BURSTware [11] The LDA measurement technique was first validated by theoretical results and hot wire data made in a single free jet at 15 nozzle widths downstream from the nozzle plate [12].

Flow visualisation Laser sheet flow visualisation using smoke and wall surface flow visualisation using oil film were employed to study the flow field. In the laser sheet flow visualisation experiments, smoke was introduced into the jet settling chamber and a horizontal laser sheet provided by the LDA laser beam with a 5mm diameter glass cylinder was used to illuminate the flow field. Wall surface flow visualisation experiments were used to determine the reattachment length for small β. The oil was made from a mixture of kerosene, titanium dioxide and a few drops of oleic acid. The ratio of titanium dioxide to kerosene was approximately 1:5 by volume and the mixture was painted along the wall surface from the wall nozzle to some distance downstream which covered the reattachment length. The direction of the oil flow depends on the pressure gradient and the wall shear stress of the working fluid. By observing the movement of the oil particles and the subsequent oil flow pattern, the reattachment length can be deduced.

RESULTS AND DISCUSSIONS

Initial Conditions

It is well known that the spatial development of free shear flows is dependent on the initial conditions [13]. For an inclined wall jet, initially at the nozzle exit, there are two distinctive boundary layers: the inner and the outer shear layers. Fig. 3 shows the mean streamwise velocity profiles measured by a single hot-wire in the two initial boundary layers at X/h=0. It can be seen that the differences between the inner and outer boundary layers velocity profiles are not significant. The shape factor is 2.85. The initial momentum thickness θ_o for $\beta = 30°$ and 90° (free jet) was measured by a single hot-wire when the nozzle exit Reynolds number was varied from 3,000 to 10,000. As shown in Fig.4, the initial momentum thickness for the free jet (90°) is proportional to $(U_o)^{-1/2}$, in agreement with published results [14, 15] and the results for β=30° also obeys the same relationship.

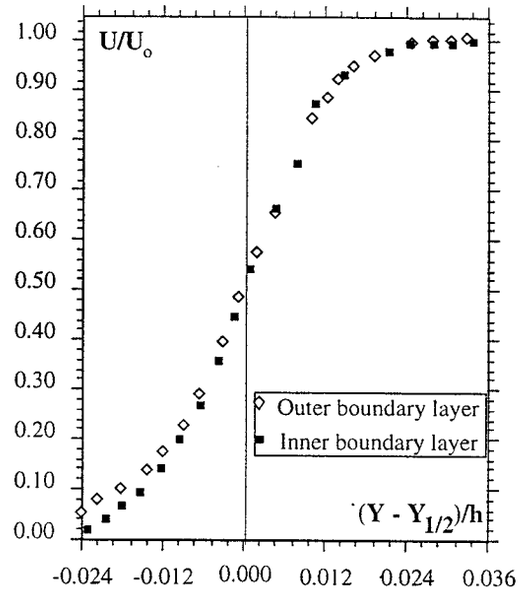

Fig. 3 Mean streamwise velocity profiles at the nozzle exit.

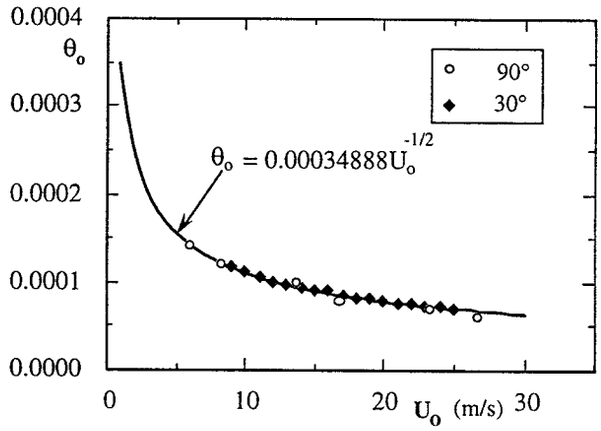

Fig. 4 Variation of the initial momentum thickness θ_o with the nozzle exit velocity.

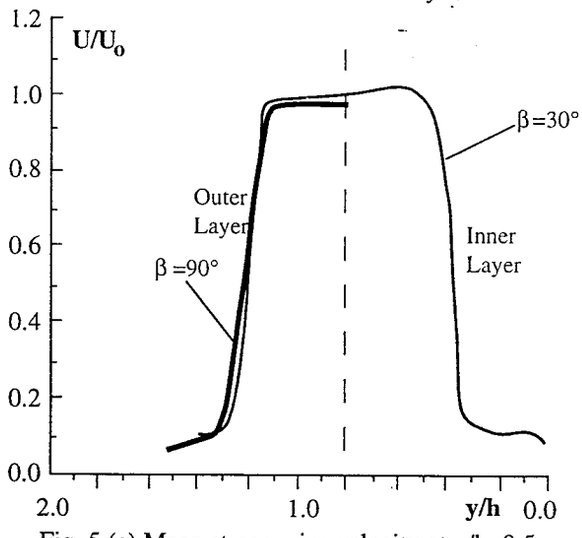

Fig. 5 (a) Mean streamwise velocity at x/h=0.5.

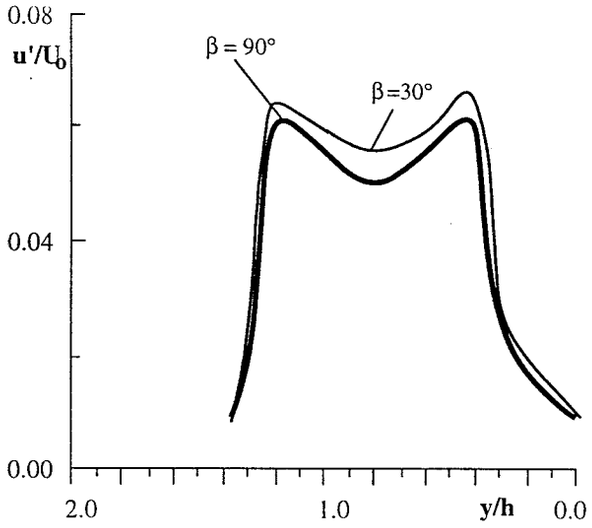

Fig. 5 (b) Streamwise turbulence intensity at x/h=0.5.

The mean streamwise velocity and turbulence intensity profiles measured by LDA at x/h=0.5 for $\beta = 30°$ are shown in Figs. 5(a) and (b) respectively. The corresponding profiles for a free jet ($\beta = 90°$) are also included for comparison. Unlike free jets which have top-hat velocity distributions in the potential core, the inclined wall jet has inclined velocity distributions near the nozzle exit, indicating that the jet is deflected towards the wall. This is known as the Coanda effect which may be explained as follows. As the jet leaves the nozzle, the fluid which is entrained in the confined region between the jet and the wall is accelerated near the wall and since the flow is two-dimensional, a pressure lower than that of the surroundings is produced on the wall. Consequently the jet curves towards the wall and reattaches to the wall if the wall is long enough.

Effect of Reynolds number

In order to determine the effect of Reynolds number, the long-time averaged reattachment position was determined by using LDA with at least 20,000 bursts for various Reynolds numbers R_0 (6,670, 10,000 and 13,340). The wall angle β was varied from 27° to 55°. Fig. 5 shows that although some data scatter is observed for $\beta > 50°$, the results obtained here are in good agreement with Newman's results [4]. Furthermore, the reattachment length is virtually independent of R_0 for $6{,}670 \le R_0 \le 13{,}340$ and $\beta < 50°$.

Effect of nozzle aspect ratio

Perry [6] re-examined the Newman's model [4] for two-dimensional jet reattachment. His experimental data for an inclined wall jet with offset demonstrated that the reattachment length is unaffected by the nozzle aspect ratio for ratios between 10 and 100 if the reattachment length x_r is normalised by the jet nozzle width h. In their studies of backward-facing step flow, Bradshaw & Wong [16] found that the effect of the nozzle aspect ratio on the reattachment length was negligible for aspect ratios greater than ten. For aspect ratios less than ten, the reattachment length for backward-facing step flows increases if the boundary layer at separation is laminar, and decreases when turbulent. To observe the effect of nozzle aspect ratio on the reattachment length, two nozzles were used with h = 5mm and 10mm but both were of the same length l (300mm), giving an aspect ratio of 60 and 30 respectively. Fig. 6 shows the variation of the reattachment length with the two different nozzle aspect ratios at R_0 = 10,000. Except for large β (> 47°), the reattachment length is virtually independent of l/h, thus indicating that for l/h ≥ 30, the jet is essentially two-dimensional even without side plates installed.

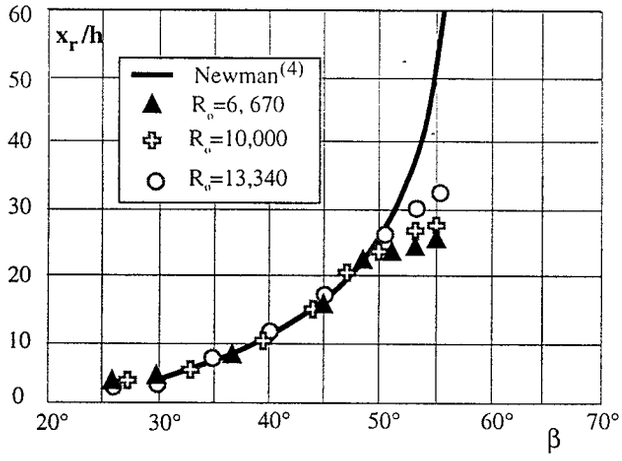

Fig. 5 Variation of x_r/h with β for various R_0.

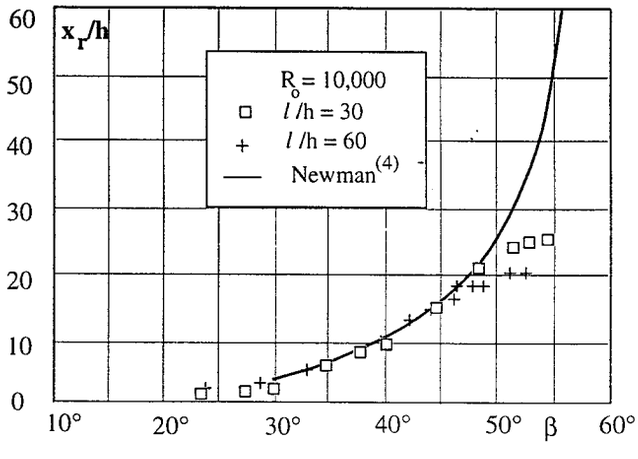

Fig.6 Variation of x_r/h with β for different nozzle aspect ratios.

Comparisons of reattachment length

The reattachment lengths determined for various β at a nozzle exit Reynolds number of 10,000 using wall surface oil film flow visualisation technique and LDA are shown in Fig. 7. It can be seen that there is good general agreement between the results which appear to follow the experimental data of Newman [4] as well.

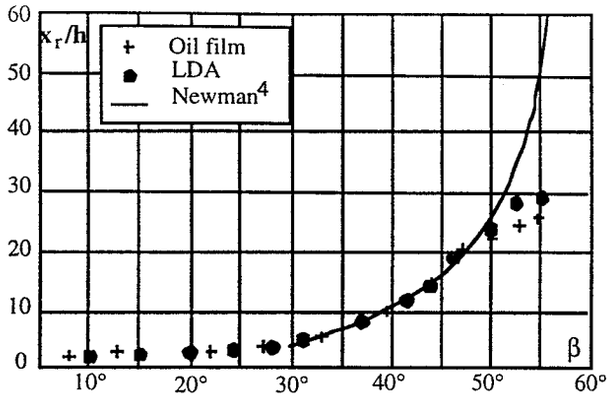

Fig. 7 Comparisons of the reattachment length determined by different methods.

Mean Velocity Field

Fig. 8 displays the general flow pattern of a 30° inclined wall jet by injecting smoke at the lips of the nozzle and illuminating it with a laser sheet. The general features of an inclined wall jet, such as the inner shear layer, the outer shear layer and the recirculation flow region as shown schematically in Fig. 1, can be discerned in Fig. 8. It can be seen that the jet is separated from the wall as soon it leaves the nozzle, then curves towards the wall and reattaches to it at some distance downstream. Further downstream the jet develops into a wall jet flow.

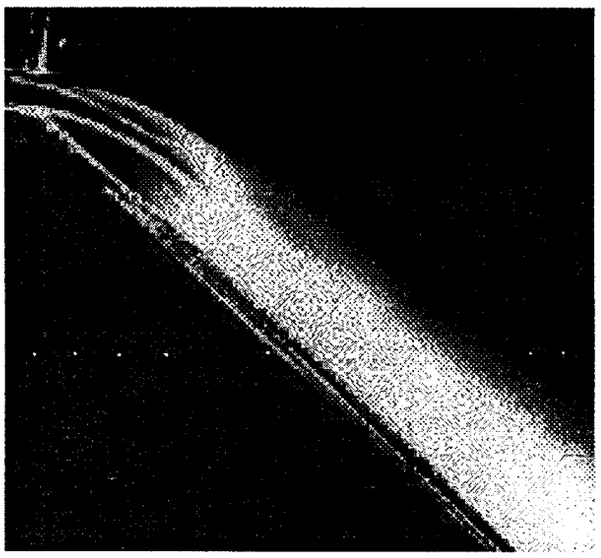

Fig. 8 Flow pattern of a 30° inclined wall jet.

Mean streamwise and transverse velocity profiles measured by X-wire and LDA at various streamwise distances (x) are shown in Figs. 9(a) and (b) respectively. It can be seen from Fig.9(a) that the mean streamwise velocity profiles measured by LDA near the wall for x/h≤6 are negative, thus indicating reversed flow and the presence of a recirculation flow region as observed in Fig. 8. It can be noted that except in the recirculation flow region where hot-wires cannot discriminate against reversed flow, there are only sight differences between the hot-wire and LDA results in the mean streamwise velocity profiles. Generally speaking, the mean streamwise velocities measured by hot-wires in the outer shear layer are slightly higher than those obtained by LDA. Both the hot-wire and LDA results indicate that the jet reattaches to the wall near x/h=6 and has developed into a wall jet flow by x/h=10.

As shown in Fig. 9(b), the mean transverse velocity profiles as measured by HWA and LDA are very similar. Initially for small x/h, V is positive, but turns to negative when the flow approaches the reattachment point, and finally becomes positive further downstream of the reattachment point. The sign of V indicates the changes in the flow pattern. Negative V indicates that the flow is curving towards the wall.

Recirculation Flow Region Fig. 10 displays the mean velocity vectors constructed from the mean and transverse velocities determined by LDA in the recirculation flow region. The reversed flow region covers the initial area in the vicinity of the nozzle exit bounded by the wall, the nozzle plate and the inner shear layer. High reversed flow velocity occurs just upstream of the reattachment point where there is high momentum transfer. The local maximum reversed flow velocity decreases as the fluid flows upstream in the recirculation flow region. It is interesting to note that the location of the maximum reversed flow velocity is shifted away from the wall surface as the flow reverses from the reattachment point. The reversed flow velocity gradient near the wall is highest just upstream of the reattachment point and then deceases as x decreases. It can be determined from Fig. 10 that the time averaged position of the reattachment point is located at $x/h \approx 6.2$. The unsteady nature of the reattachment point is illustrated by monitoring the short-time averaged velocity vector at x/h=6 for 300 secs as shown in Fig. 11. It is quite obvious that the direction of the short-time averaged velocity vector changes substantially with time.

Maximum streamwise velocity decay Fig. 12 displays the decay of maximum streamwise velocity with x/h for $\beta = 0°$ (wall jet), 30° and 90° (free jet). It can be seen that for the inclined wall jet, the local maximum velocity U_m in the vicinity of the nozzle is higher than the nozzle exit velocity U_o. This is due to the existence of a recirculation flow region where the pressure is lower than the ambient pressure, consequently accelerating the flow in the inner shear layer. Moreover, the potential core length of the inclined wall jet is considerably shorter than that of the free jet and wall jet, accompanied by a much faster rate of the initial decay of U_m. This is a direct result of the Coanda effect whereby the jet is deflected towards the wall. By x/h=10, the decay rate of U_m for the 30° inclined wall jet approaches that of the 0° wall jet.

Jet spreading Fig.13 displays the spatial distribution of the jet half-width ($y_{1/2}$) in the outer shear

layer, ($y_{-1/2}$) in the inner shear layer and the location (y_m) of maximum local streamwise velocity. The influence of the recirculation flow region on the inner shear layer half-width of the jet can be easily identified.

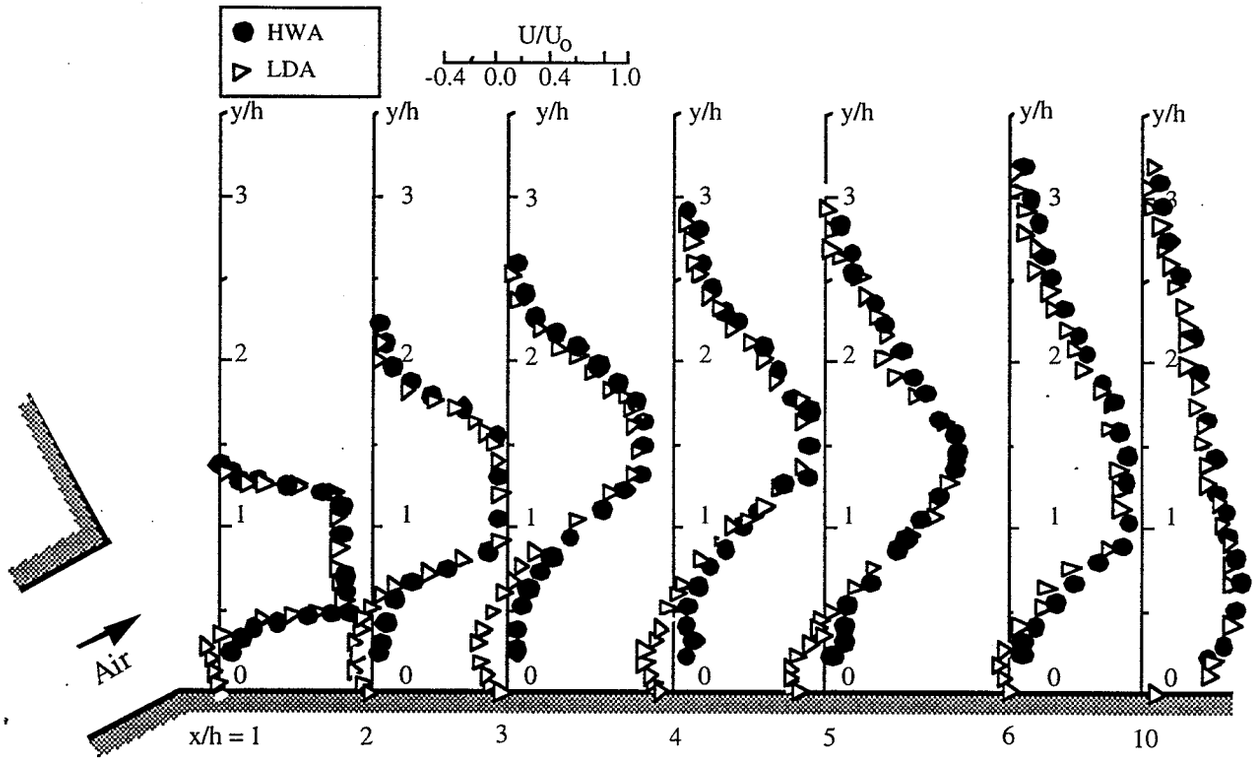

Fig. 9(a) Mean streamwise velocity profiles.

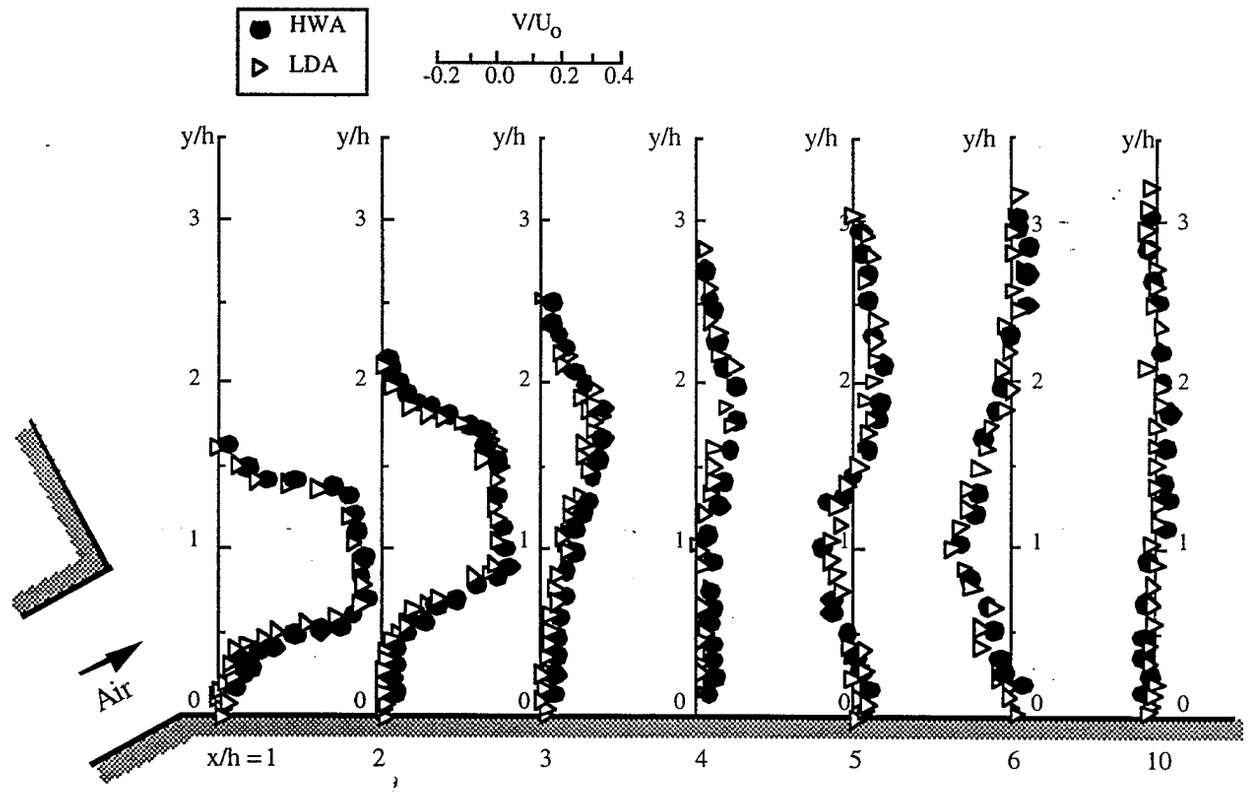

Fig. 9(b) Mean transverse velocity profiles.

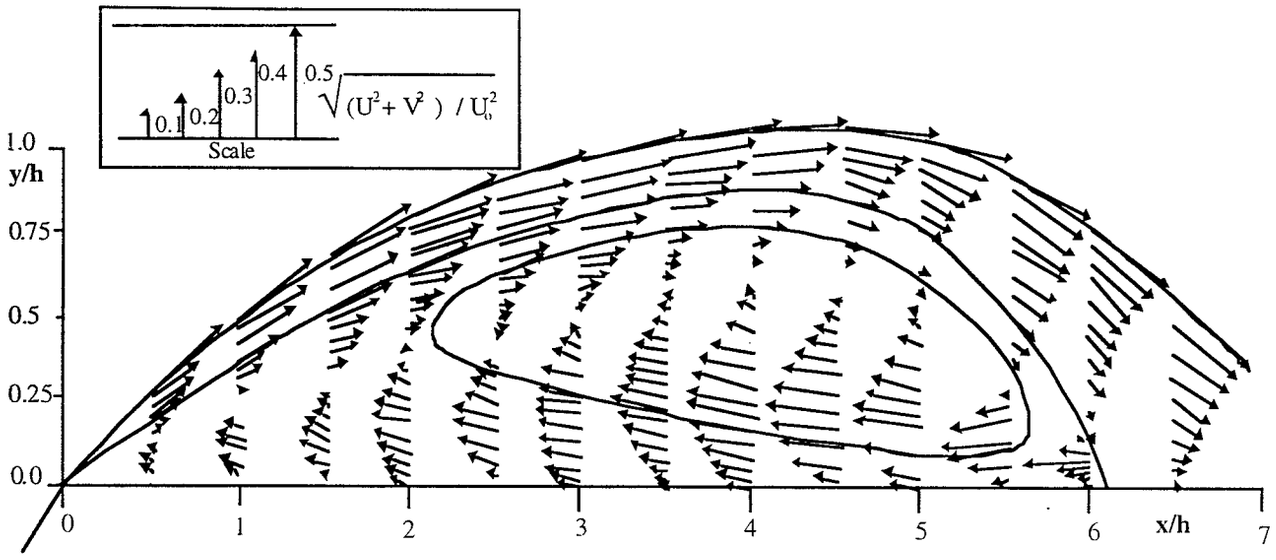

Fig. 10 Mean velocity vectors in the recirculating flow region.

Turbulence field

Turbulence intensities The spatial development of streamwise and transverse turbulence intensities (u'/U_o and v'/U_o) in the x- and y-directions obtained by X-wire and LDA is displayed in Figs. 14(a) and (b) respectively. No significant differences between the LDA and HWA measurements can be observed. The turbulence intensity distributions exhibit two peaks in u' and v', which are associated with the inner and outer shear layers. Moreover, for $x/h \leq 5$, the peak of u'/U_o in the inner shear layer is higher than that in the outer shear layer whereas the peak of the transverse turbulence intensity distributions v'/U_o in the outer shear layer is higher than that in the inner shear layer. This is because the flow is constrained in the inner shear layer in the y-direction, and the flow in the outer shear layer is relatively "free".

Reynolds shear stress distributions Comparisons of the spatial development of Reynolds stress $-\overline{uv}/U_o^2$ measured by LDA and HWA are made in Fig. 14(c). There are no significant differences between the HWA and LDA measurements. Similar to the turbulence intensity profiles, the inner and outer shear layers can be identified by the peaks in $-\overline{uv}/U_o^2$. As the flow proceeds downstream, large negative values of $-\overline{uv}/U_o^2$ can be identified near the wall, characterising the momentum transfer between the inner shear layer and the recirculation flow region. The magnitude of the Reynolds shear stress reaches a maximum value in the vicinity of the reattachment point, indicating high momentum transfer due to the jet impinging on the wall.

CONCLUSIONS

The mean velocity and turbulence field of a 30° inclined wall jet has been measured using hot-wire and laser Doppler anemometry for a nozzle exit Reynolds number of 6,700. The LDA results indicate that the jet is separated from the wall as soon as it leaves the nozzle but due to the subatmospheric pressure in the region confined between the wall, the nozzle plate and the inner shear layer of the jet, the jet is attracted towards the wall and reattaches to it at 6.2 nozzle widths downstream. The spatial development of the inner and outer shear layers and the recirculation flow region as revealed by smoke flow visualisation is quantified by the LDA data. Comparisons between the hot-wire and LDA measurements indicate that with the exception of the recirculation flow region where hot-wires cannot discriminate reversed flow, the results are very similar. The unsteady nature of the reattachment point has been illustrated by the time variation of the short-time averaged velocity vector in the vicinity of the reattachment point. Reattachment lengths determined by LDA measurements show that for $\beta < 50°$, they are virtually independent of the nozzle aspect ratio provided that it is greater than 30. Furthermore, the reattachment length is independent of the Reynolds number range 6,670 - 13,340 provided that β is less than 50°.

ACKNOWLEDGMENT

D. Lu acknowledges receipt of a University College Rector's scholarship for undertaking this study.

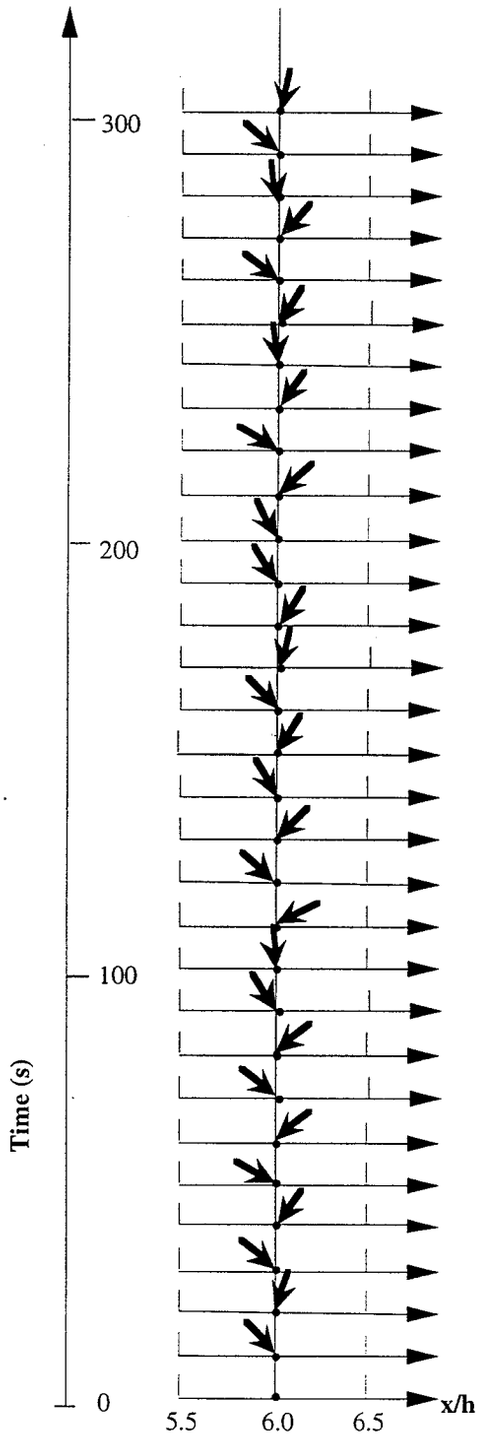

Fig. 11 Variation of the short-time averaged mean velocity vector with time at x/h=6.

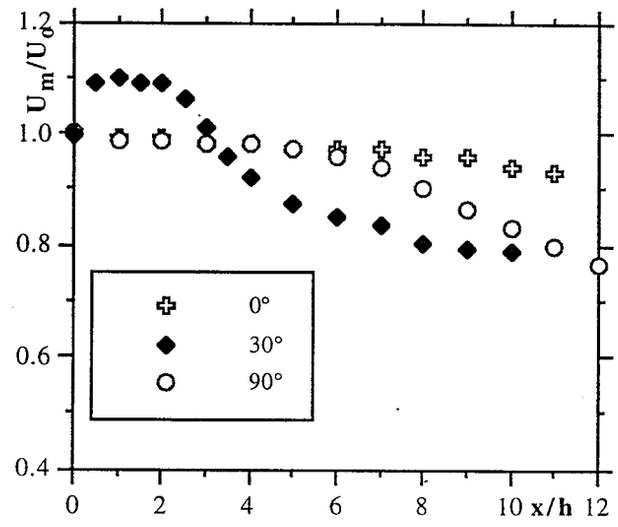

Fig. 12 Variation of maximum streamwise velocity with x/h.

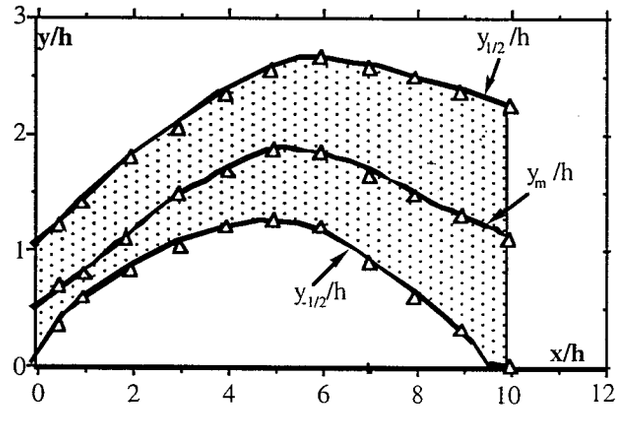

Fig. 13 Variation of trajectories of jet halfwidths and maximum local streamwise velocity with x/h.

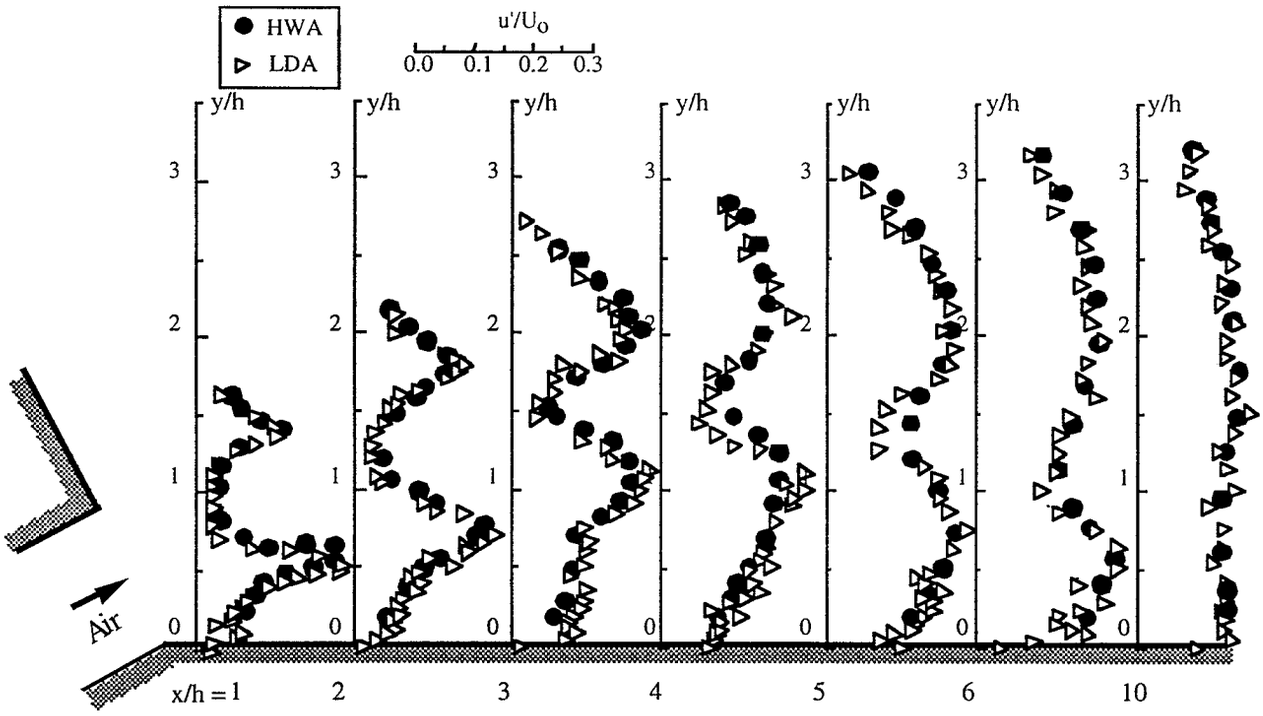

Fig. 14(a) Streamwise turbulence intensity profiles.

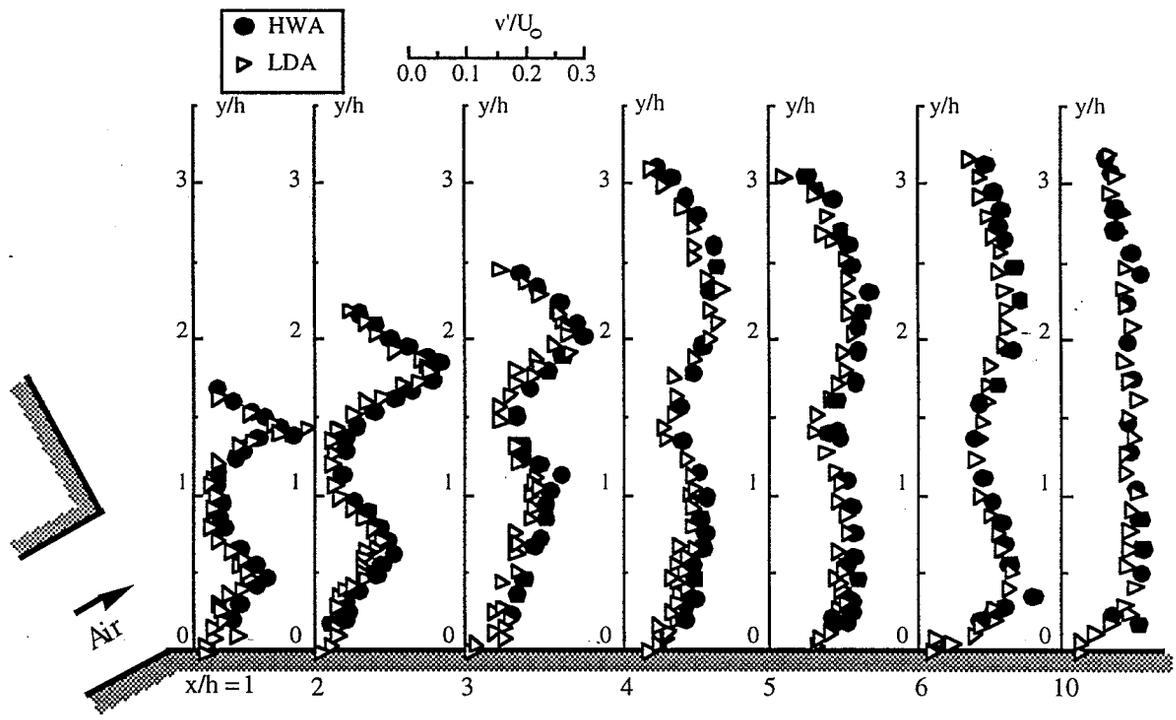

Fig. 14(b) Transverse turbulence intensity profiles.

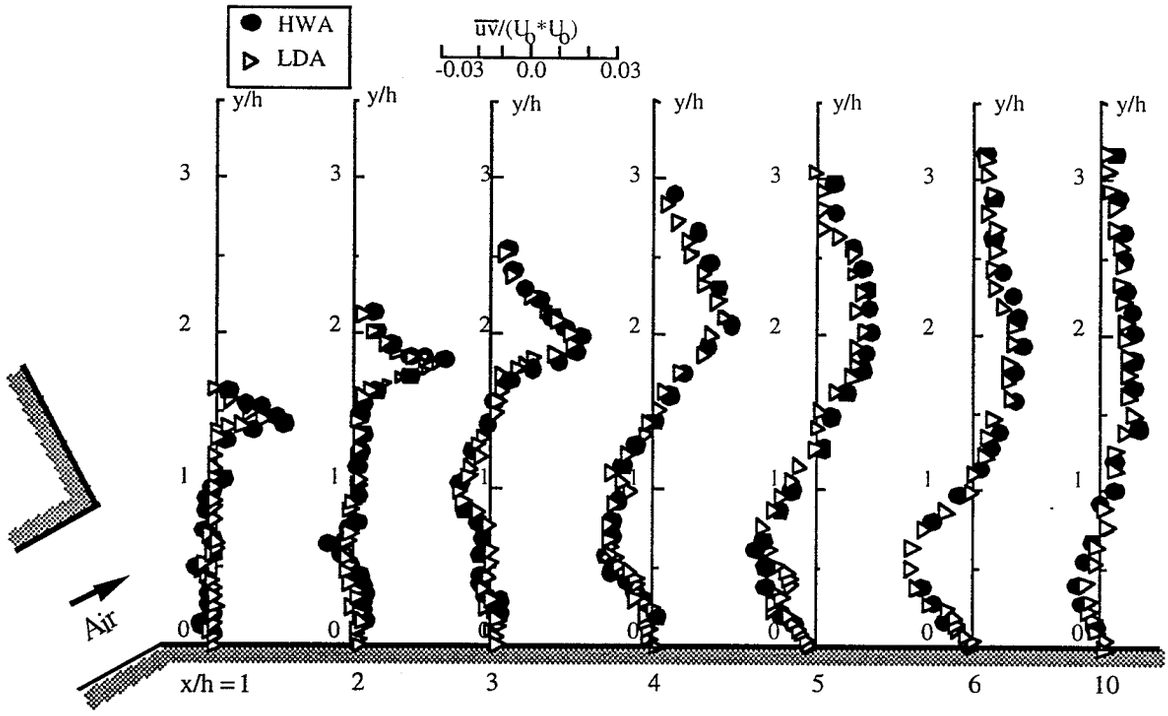

Fig. 14(c) Reynolds shear stress profiles.

REFERENCES

1. Launder, B.E. & Rodi,W. (1981) *The turbulent wall jet.* Prog. Aerospace Sci. **19**, 81-128.
2. Forthmann,E. (1934) *Uber Turbulente Stranhlausbreitung.* Ing-Arch., **5**, 42.
3. Sproule, R.S., Adderley, J.W. & Robinson (1944) *The Coanda Effect.* S.T.C.I.O.S., S.H.A.E.F. Item No. 5 .
4. Newman, B.G. (1961) *The deflection of plane jet by adjacent boundaries - Coanda effect.* Boundary Layer and Flow Control (ed. G.V. Lachmann), Pergamon Press **1**: 232 - 265.
5. Bourque, C. (1967) *Reattachment of a two-dimensional jet to an adjacent flat plate.* Advances in Fluidics (ed. F.T. Brown), ASME, 192 - 204.
6. Perry, C.C. (1967) *Two-dimensional jet attachment.* Advances in Fluidics (ed. F.T. Brown), ASME, 205 - 217.
7. Lai, J.C.S. & Lu, D. (1996) *Effect of wall inclination on the mean flow and turbulence characteristics in a two-dimensional wall jet.* Int. J. Heat & Fluid flow **17**(4), 377-385 (1996).
8. Lai, J.C.S. & Lu, D. (1992) *An inclined two-dimensional wall jet.* Proc. 5th Asian Congress of Fluid Mechanics, **1**, 195-98.
9. British Standards Institution (1973) *Methods for measurement of fluid flow in pipes.* BS1042 Part 1.
10. Lai, J.C.S. & Simmons (1985) *Instantaneous velocity measurements in a vane-excited plane jet.* AIAA J, **23**(8), 1157-1164.
11. Burstware (1991) *Burstware manual.* Dantec Elektronik, Denmark, 177 pp.
12. Lu, D. (1994) *Inclined wall jets.* PhD thesis, The University of New South Wales.
13. Hussain, AKFM (1978) *Initial condition effect on free turbulent shear flows.* Lecture Notes in Physics, **76**, 1-9.
14. Gutmark, E. and Ho, C.M. (1983) *Preferred modes and the spreading rates of jets.* Physics Fluids, **26**(10), 2932-2943.
15. Hsiao F.B. and Huang, J.M. (1990) *On the evolution of instabilities in the near field of a plane jet.* Physics Fluids, **A2**, 400-412.
16. Bradshaw, P. and Wong, F.Y.F. (1972) *The reattachment and relaxation of turbulent shear layer.* J. Fluid Mech., **52**, 113-135.